

BioSET - Biomarker-based Spatial co-Expression analysis in Tumor environments

Chahat Kalsi¹ * Yuancheng Shen¹ Sophia Gaupp² Luca Reichmann² Meri Rogava⁵ Michael Krone⁴ Saeed Boorboor³ Robert Krüger¹ ,

¹ New York University ²University of Tübingen ³University of Illinois Chicago

⁴ Stuttgart University of Applied Sciences ⁵Zucker School of Medicine at Hofstra/Northwell

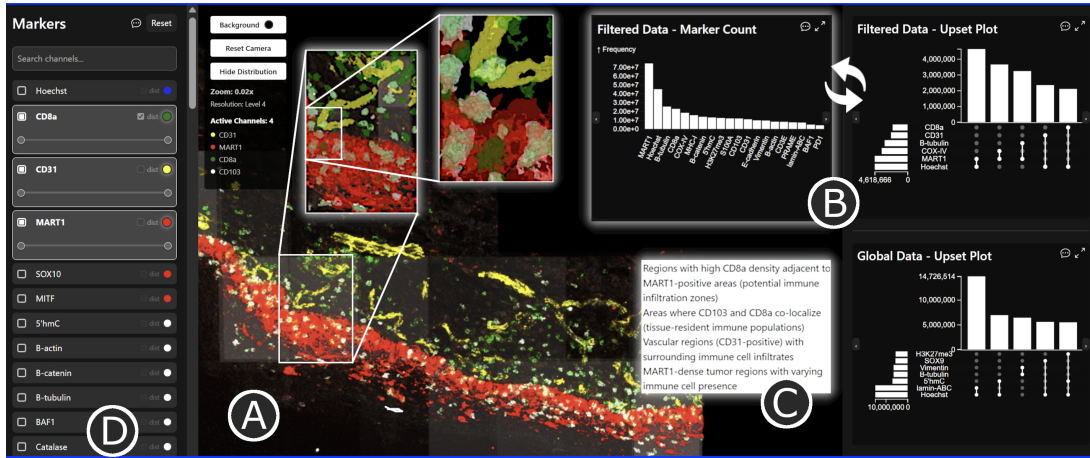


Figure 1: **BioSET.** (A) Multi-volume rendering of selected protein channels with distance-adaptive resolution. T-cells (CD8a, green), are migrating out of blood vessels (CD31, yellow) to infiltrate and fight melanoma cells (MART1, red); a tile-based heatmap (gray) guides users to regions with high co-location of these protein markers. Hierarchical regional selections reveal details on cellular scale with combined mesh+volume rendering: Presence of CD103 (white) suggests that some t-cells are ‘tissue-resident’, rather than entering from the bloodstream. (B) UpSet plots summarize frequencies of most intersecting channel sets both globally and for the selected markers. Plots can also be toggled to individual channel-wise counts. (C) Biomni AI agent provides textual interpretation. (D) Selection of channels and visualization parameters.

1 INTRODUCTION

This abstract reports on our solution to the IEEE VIS 2025 Bio+MedVis 3D Microscopy Imaging Challenge with the tasks of identification and visualization of cellular (immune-tumor) interactions in 3D Cyclic Immunofluorescence (CyCIF) data. The provided 3D melanoma tissue data [11] comprises 70 channels (volumes) across 6 levels of resolution, the highest having $194 \times 5,508 \times 10,908$ voxels per channel (1.48 TB) and the lowest having $194 \times 172 \times 340$ voxels per channel (1.48 GB).

For this dataset, the challenge defined **three tasks**: (**T1**) Detect ROIs containing user-specified bio-marker combinations; (**T2**) Visualize these ROIs globally to assess extent and tissue context; (**T3**) Enable cellular-level drill-down within selected ROIs.

Few (mostly proprietary) existing tools such as Imaris [5] can visualize multi-volumetric data at scale, and being visual display-focused, their spatial analysis capabilities are limited to manual exploration. While integrated analytics approaches, e.g., [10], have been proposed for 2D multiplexed imaging data, methods that handle volumetric datasets are rare. Most related to our work is Cell2Cell by Mörth *et al.* [6], a novel segmentation-free approach that assumes equally sized spherical cells and is evaluated on small volumes of resolution $55 \times 1,024 \times 1,024$. By contrast, our approach scales to

much larger data and is able to account for diverse cell shapes.

In summary, our approach makes the following **contributions**: (**1**) a method to detect protein-expressing regions and identify spatially co-located marker sets in the tissue. (**2**) A scalable overview-detail visualization, combining multi-scale volume and surface rendering, to guide users to regions of interest, and (**3**) integrated contextual querying, providing semantic explanations of displayed patterns. We analyzed the data using our tool in joint sessions with a biomedical expert (co-author) from *Northwell Health, New York*; the findings reported in the abstract and the supplemental materials stem from these sessions, aligning with manual analyses by experts [11].

2 APPROACH

Identification of Marker Sets For **T1**, we use a set-based method to detect regions of marker co-expression. We use the iso-value selection method of Pekar *et al.* [7] to find out which voxels capture the markers expressed in each channel. Since the detected iso-value τ is more accurate in a local context than globally, we process the volume in $194 \times 1377 \times 909$ tiles at the finest resolution level. We then threshold each tile per channel at $I \geq \tau$ to obtain masks that approximate marker-expressing voxels (Fig. 2 (i)).

Subsequently, we compute the intersections between channels. Voxels that are marked as ‘ON’ in the binary mask at the same spatial location across tile masks corresponding to each channel are being co-expressed. Lastly, we perform these calculations for finer-grained tiles of resolution $194 \times 459 \times 303$ and use the results to visualize the hotspots in Fig. 4 and in the drill-down view visible in Fig. 1 (A).

Hybrid Multi-Volume and Surface Rendering To provide overview, we visualize the data globally (**T2**, Fig 1 (A)). Given the

*corresponding (first) author: Chahat Kalsi, chahat.kalsi@nyu.edu — Second authors Shen, Gaupp, and Reichmann contributed equally.

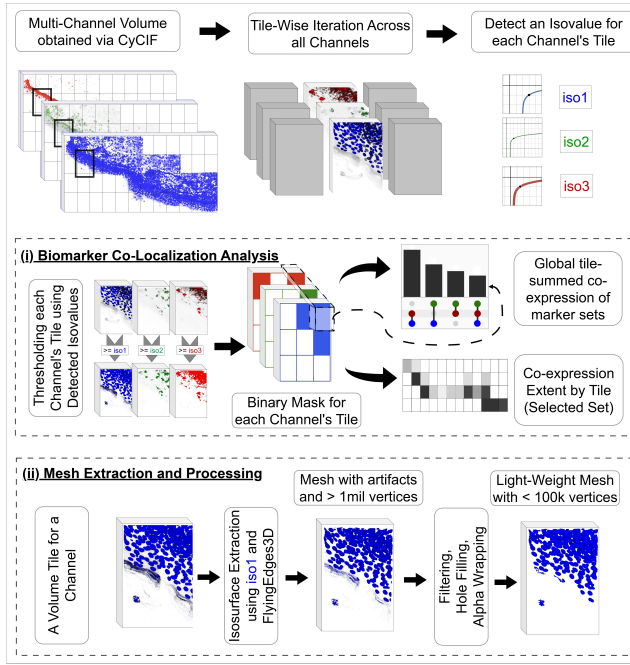


Figure 2: Processing and Analysis Pipeline. We iterate the multi-channel volume tile-by-tile and estimate a per-channel iso-value for each tile. We use this iso-value for (I) Biomarker Co-Location Analysis and (ii) Mesh Extraction and Processing.

6 resolution levels in the dataset, we built a web-based multi-scale volume renderer based on VTK.js [8], capable of switching between resolutions based on camera distance from the volume center. In practice, it can render resolution levels 4-6 and support up to seven channels simultaneously. To explore the data interactively, users can search and select channels of interest from a marker list (Fig. 1 (D)), assign them colors and adjust their intensity ranges. Additionally, a preselected interaction section below allows selection of marker groups whose spatial overlap indicates a specific biological context (e.g., immune cells).

While volume rendering is sufficient for global views, it can be difficult to demarcate the boundaries of expressed markers on a cellular level (T3). This is due to the often diffuse protein marker distribution. To achieve a clearer view of regions with expressed markers, we employ surface rendering. To derive the surfaces (Fig. 2 (iii)), we first extract per-channel meshes for each of the $194 \times 1377 \times 909$ tiles using the *FlyingEdges3D* [9] algorithm with the previously detected iso-values τ . We then perform a series of processing steps (Fig. 2 (ii)) on the raw meshes obtained through this. We, (i) drop connected components below a face-count threshold, (ii) fill small holes using mean component diameter and face count statistics [2], (iii) apply *alpha-wrapping* with parameters derived from the mean component diameter [1], and (iv) remove residual noisy components by face count. The result is a clean, low-polygon mesh per tile and channel for interactive, cell-level inspection.

Guidance to Regions of Interest To visualize which sets of markers frequently spatially overlap, we integrate two interactive UpSet plots [4], as shown in Fig. 1 (B). In Fig. 1 (B), the global plot displays the overall marker abundances and co-localizations across the whole dataset, while the filtered plot is updated dynamically based on the current marker selection. The UpSet plots (Fig. 1 (B)) and the viewer (A) are linked: selecting markers updates the view, while current channel selections in the viewer highlight the corresponding sets in the filtered UpSet plot. As the plot can get cluttered as the number of channels grows, we provide an additional

filtering feature to only include markers of interest in the plot.

To guide users to regions with prominent interactions (T2), we overlay the volume with a tile-level co-expression heatmap: each $194 \times 1137 \times 909$ tile is colored by the count of co-expressing voxels for the selected group (white = high; black = low with reduced opacity), revealing global ROIs. We use grayscale to avoid interfering with channel colors. Selecting a tile opens a drill-down with combined volume+mesh rendering and a sub-tile heatmap at $194 \times 459 \times 303$, guiding users to cell-scale structures (T3). As a coarse heatmap can miss small interaction “hotspots”, we also compute ROIs at the finer $194 \times 459 \times 303$ tile-size and visualize them as circles of varying radii in the main view (Fig. 4).

Contextual Queries for Biomedical Explanations To aid the interpretation process, we integrate semantic textual explanations using Biomni [3]. Biomni is an AI agent designed to perform domain-specific reasoning on biomedical data. Explanation buttons send targeted queries to Biomni together with their relevant context. The output (Fig. 1 (C)) summarizes what is visible, explains its biological relevance, suggests ROIs, and offers an assessment of possible clinical relevance. This is valuable for cases where the significance of markers and their combinations is not immediately apparent, particularly to non-specialists.

3 DISCUSSION AND FUTURE WORK

Our solution draws on a hierarchical subdivision (tiling) of the multi-volume data to identify co-located protein markers and a combined volume and surface rendering from overview to detail. Current limitations thus lie in the artificial spatial binning and the level of detail. In the future, we aim to leverage cell segmentation to identify spatial patterns on a cellular basis and to integrate steerable deep-learning for scalable feature-based ROI classification and search.

REFERENCES

- [1] P. Alliez et al. “3D Alpha Wrapping”. In: *CGAL User and Reference Manual*. 6.0.1. CGAL Editorial Board, 2024.
- [2] D. Coeurjolly et al. “Polygon Mesh Processing”. In: *CGAL User and Reference Manual*. 6.0.1. CGAL Editorial Board, 2024.
- [3] K. Huang et al. *Biomni: A General-Purpose Biomedical AI Agent*. en. Pages: 2025.05.30.656746 Section: New Results. 06/2025.
- [4] A. Lex et al. “UpSet: Visualization of Intersecting Sets”. In: *IEEE TVCG* 20.12 (12/2014), pp. 1983–1992.
- [5] *Microscopy Image Analysis Software - Imaris - Oxford Instruments*. imaris.oxinst.com, last accessed: 08/22/2025.
- [6] E. Mörth et al. “Cell2Cell: Explorative Cell Interaction Analysis in Multi-Volumetric Tissue Data”. In: *IEEE TVCG* 31.1 (01/2025), pp. 569–579.
- [7] V. Pekar, R. Wiemker, and D. Hempel. “Fast detection of meaningful isosurfaces for volume data visualization”. In: *Proceedings Visualization, 2001. VIS '01*. 10/2001, pp. 223–230.
- [8] W. Schroeder, K. Martin, and B. Lorensen. *The Visualization Toolkit (4th ed.)* Kitware, 2006.
- [9] W. Schroeder, R. Maynard, and B. Geveci. “Flying edges: A high-performance scalable isocontouring algorithm”. In: *IEEE LDAV*. 2015, pp. 33–40.
- [10] A. Somarakis et al. “ImaCytE: Visual Exploration of Cellular Micro-Environments for Imaging Mass Cytometry Data”. eng. In: *IEEE TVCG* 27.1 (01/2021), pp. 98–110.
- [11] C. Yapp et al. *Highly Multiplexed 3D Profiling of Cell States and Immune Niches in Human Tumours*. en. Pages: 2023.11.10.566670 Section: New Results. 04/2025.

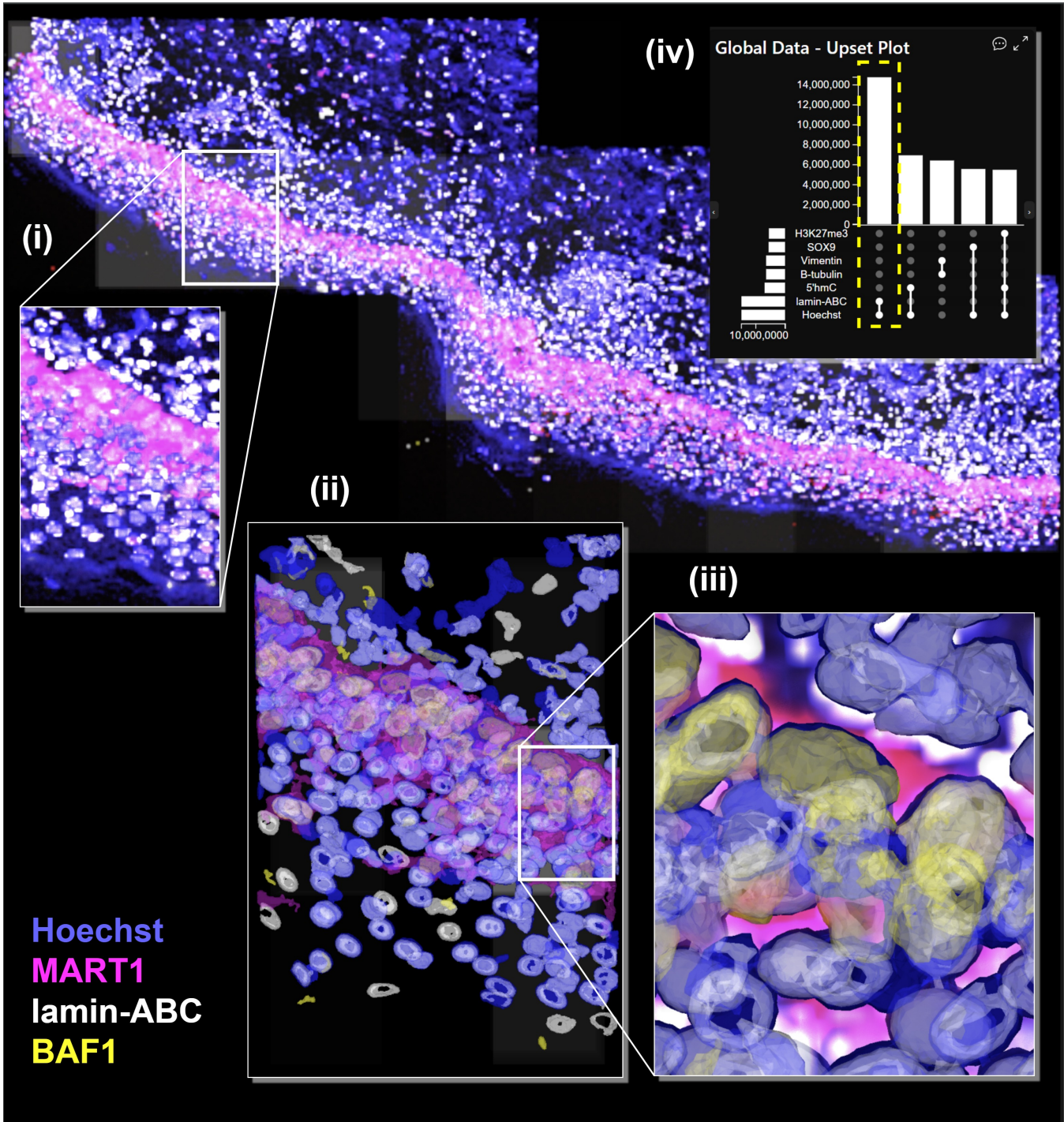


Figure 3: Potential Nuclear Envelope Rupture. The main visualization shows a volumetric rendering of the markers *Hoechst* (blue), *MART1* (magenta), *lamin-ABC* (white), and *BAF1* (yellow). The global UpSet plot in inset (iv) highlights *Hoechst* \wedge *lamin-ABC* as the most frequent pair, consistent with DNA and nuclear-lamina co-localization; *Hoechst*⁺ nuclei lacking *lamin-ABC* suggest rupture candidates. Given that *BAF1* might represent proteins present at nuclear-envelope breakage sites, we examine *Hoechst* \wedge *BAF1*: the background heatmap encodes their co-expression; (i) shows a high resolution volume rendering of a tile where this co-expression is high, (ii) shows how the mesh rendering can further enhance detail, with a sub-tile heatmap guiding us to (iii) a combined mesh and volume rendering of a cellular drill-down showing *Hoechst* \wedge *BAF1* co-expressed without *lamin-ABC* on some nuclei, which might represent a nuclear-envelope rupture. *MART1* provides tumor context.

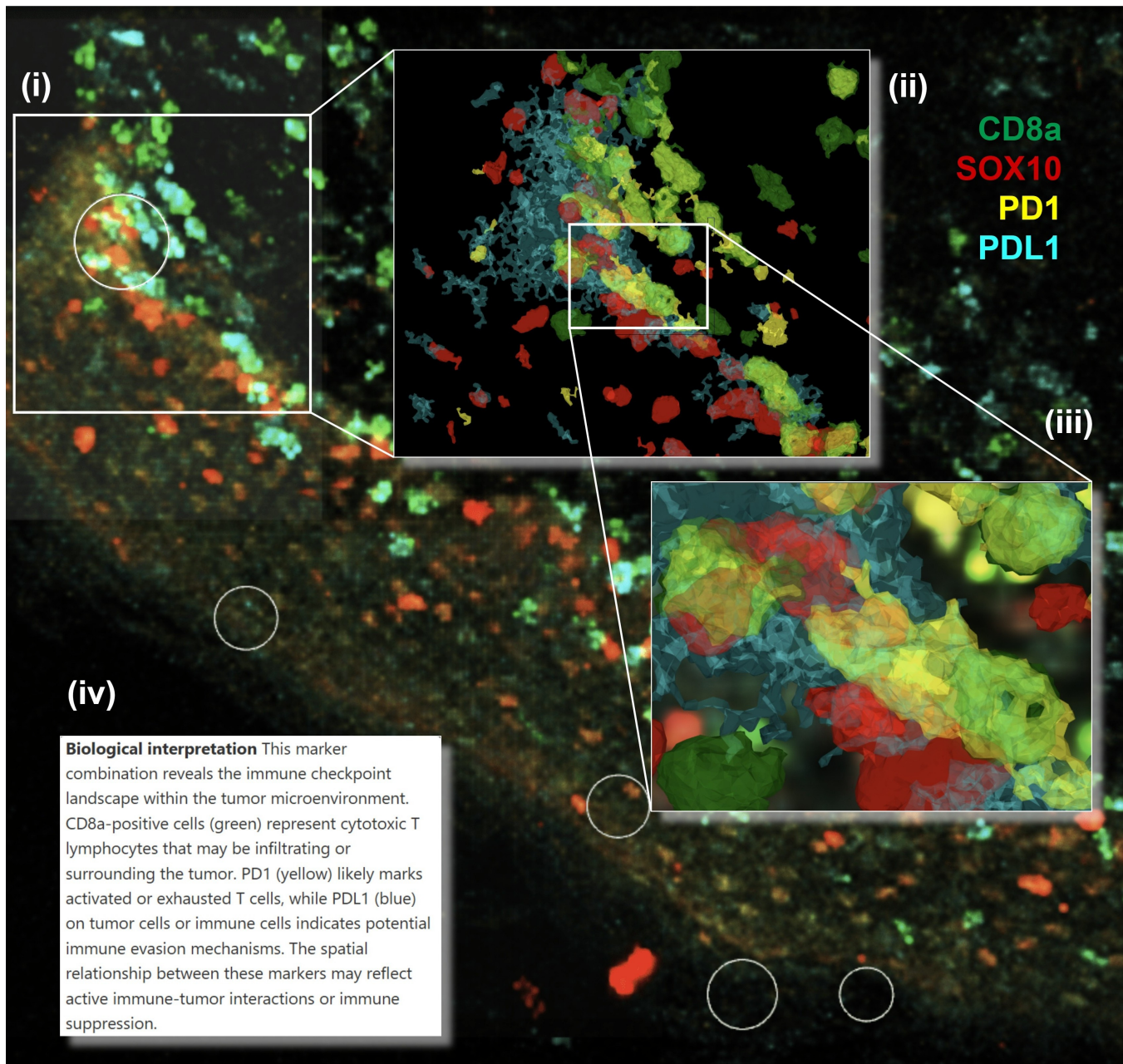


Figure 4: PD1–PDL1 checkpoint. The main view shows a volumetric rendering of *CD8a* (green; cytotoxic T cells), *MART1* (red; melanoma), *PD1* (yellow; T-cell inhibitory receptor), and *PDL1* (cyan; its ligand on tumor cells). *PD1–PDL1* binding at T-cell–tumor contacts suppresses the T-cell attack; blocking this axis is a major immunotherapy strategy. To locate potential sites, we examine *PD1–PDL1* co-location. **(i)** Circles (and the tile-level heatmap) highlight high co-location. **(ii)** In the marked area, *CD8a⁺ PD1⁺* T cells infiltrate the *SOX10⁺* tumor microenvironment with abundant *PDL1*. **(iii)** Drill-down shows a *MART1⁺/PDL1⁺* cell contacting a *CD8a⁺* T cell with *PD1* at the interface. **(iv)** Biomni provides a textual interpretation consistent with this interaction.

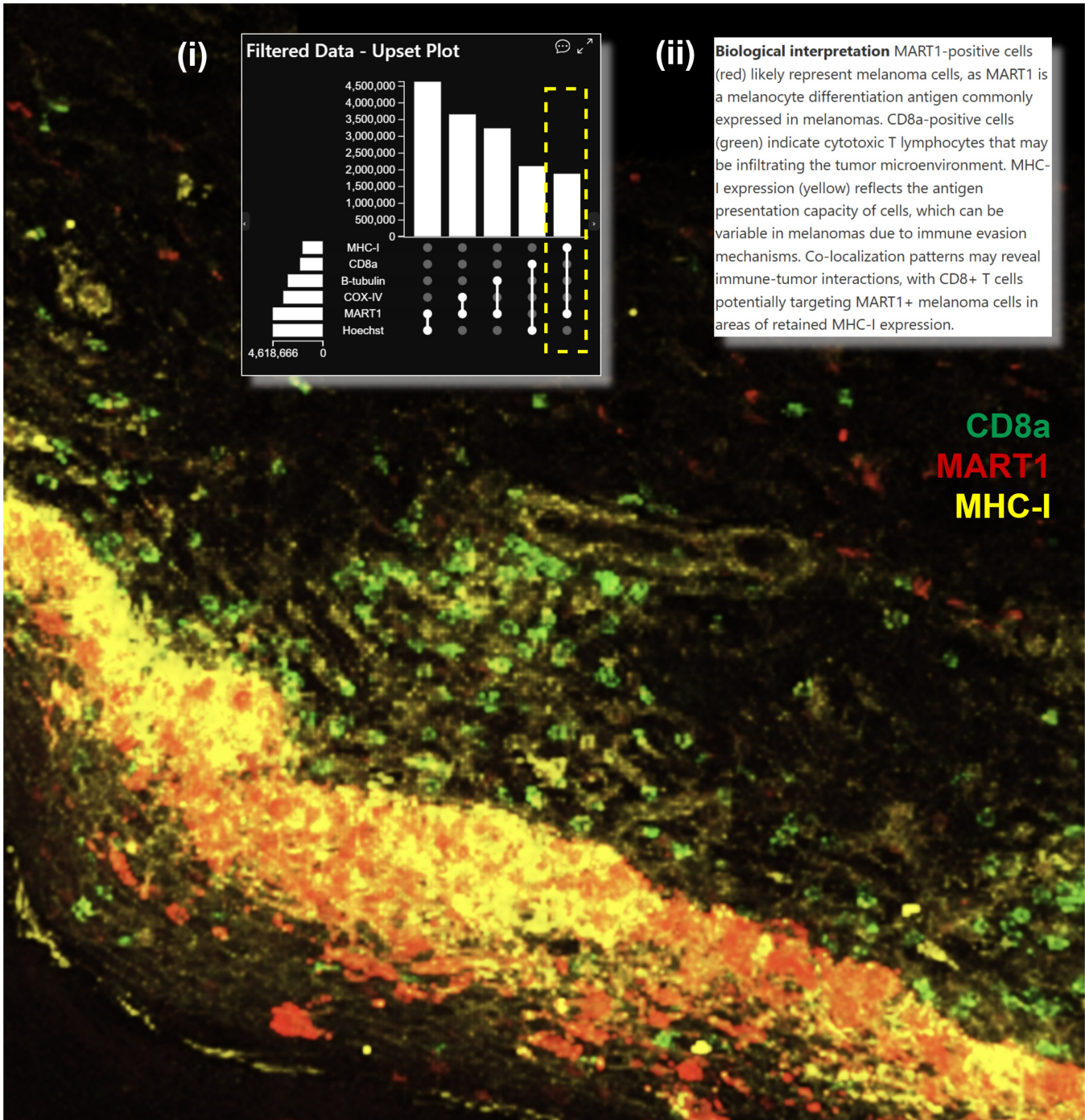


Figure 5: Antigen Presentation. The main view shows a volumetric rendering of *CD8a* (green), *MART1* (red), and *MHC-I* (yellow). *MART1* marks melanoma cells; the filtered UpSet inset (i) highlights frequent *MART1*-*MHC-I* co-occurrence, which suggests intact antigen presentation, making tumor cells visible to *CD8a*⁺ T cells. This is consistent with the observed infiltration of T-cells in the melanoma microenvironment. Biomni's explanation (ii) aligns with this interpretation.

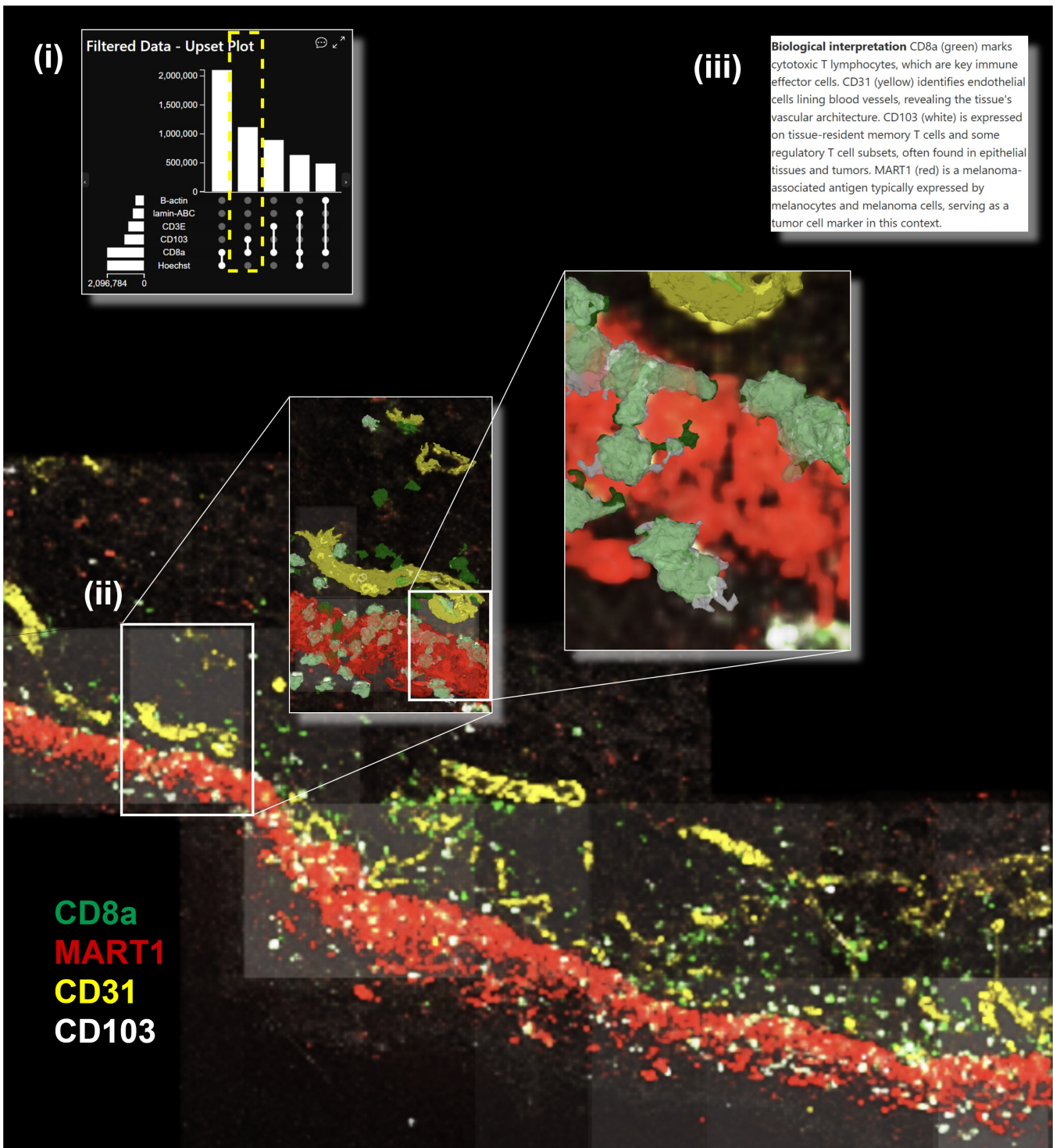
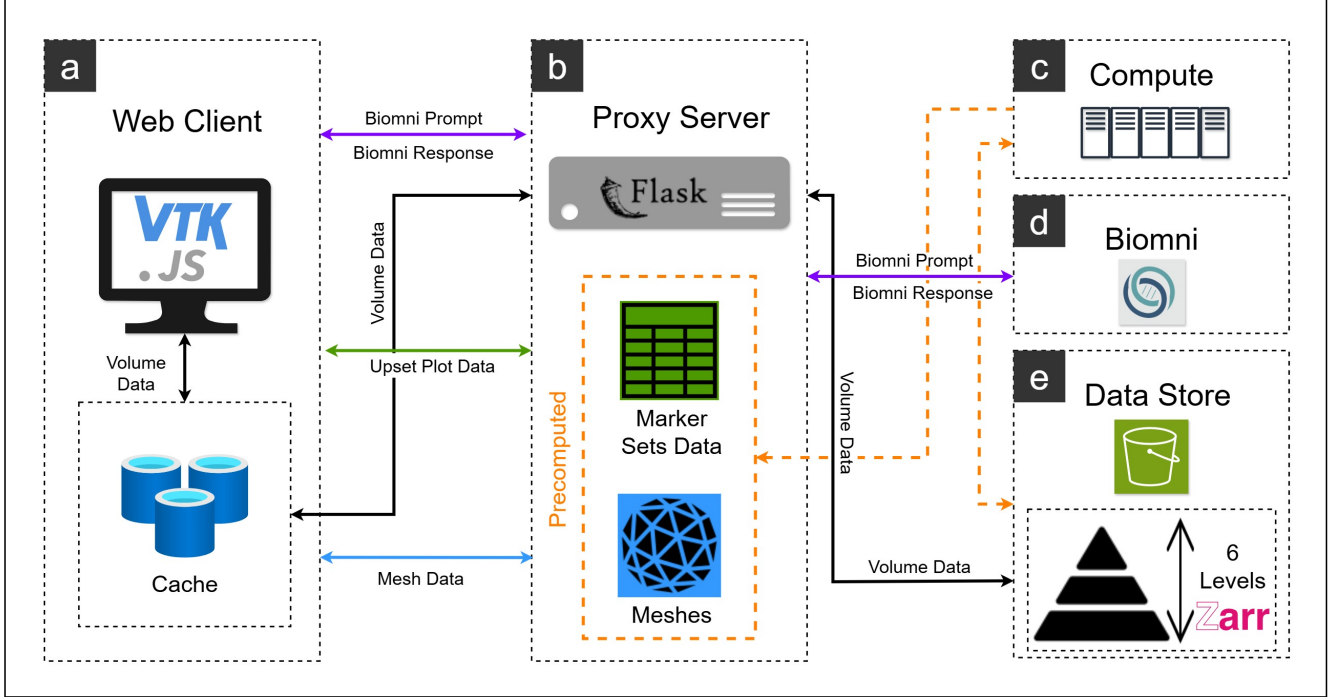


Figure 6: Tissue-Resident Memory (TRM) T-Cells. The main view shows a volumetric rendering of *CD8a* (green), *MART1* (red), *CD31* (yellow), and *CD103* (white). *CD8a* marks cytotoxic T cells, which may be intravascular (circulatory) or tissue-resident. (i) The filtered UpSet plot highlights frequent *CD8a*-*CD103* co-occurrence. *CD103*, a marker present in tissue, being co-expressed with T-cells, can indicate that the T-cells are of the TRM type. (ii) The heatmap flags a tile with high *CD8a* \wedge *CD103*, selecting which shows *CD8a* cells from the blood vessels (region near *CD31*) lacking *CD103*, while infiltrating cells in the *MART1*⁺ tumor microenvironment are *CD103*⁺. A sub-tile heatmap guides to clear co-location of *CD8a* \wedge *CD103*, where a mesh+volume rendering provides cellular-level detailed visualization of this co-expression. (iii) Biomni's explanation aligns with this interpretation.



Process	System Specifications	Small Tiles (432) (194×459×303)	Large Tiles (48) (194×1377×909)
Iso-Value Detection	Workstation (AMD Ryzen 9 8945HS, 8 cores, 32 GB RAM)	77.58 hours	35.51 hours
Co-Expression Analysis	HPC node (Intel Cascade Lake 8268, 14 cores, 96 GB RAM)	16.82 hours	3.36 hours
Mesh Extraction & Processing	Workstation (AMD Ryzen 9 8945HS, 8 cores, 32 GB RAM)	–	78.57 hours

Figure 7: BioSET System Architecture and Computational Costs. (a) Web-client with a VTK.js renderer for multi-scale volume+mesh rendering, with client side caching. (b) Flask and Python proxy server, which serves precomputed marker sets and mesh data. (e) Zarr data store on AWS S3 (6 resolution levels). (d) Biomni agent. (c) Compute resources used for offline preprocessing (mesh extraction, marker combinations calculations). **Data Pipelines.** **Black - Volume data.** The web client requests a selected channel at a resolution determined by camera distance; the proxy fetches it from the Zarr store and streams it back. Returned chunks are cached client-side for faster reuse. **Blue - Mesh data.** Per-tile, per-channel meshes are stored on the proxy. The client requests meshes for selected tiles/channels and the proxy serves the precomputed data. **Green - UpSet inputs.** Marker-set aggregates reside on the proxy. The client requests the needed subset; the proxy filters/parses and returns it. **Violet - Biomni.** User prompts from the client go to the proxy, which forwards them to the Biomni API, receives the response, parses it, and sends it back to the client. **Orange - Preprocessing.** Compute resources calculate meshes and marker-set aggregates offline, reading the volumetric data directly from the Zarr store and writing results to the proxy's storage. **Compute Resources and Computational Costs.** The 3-stage preprocessing pipeline (Fig. 2) was executed on two machines, with specifications listed in the table. Mesh extraction was performed only for the larger tile size. Reported times correspond to processing the full multi-volume dataset at the highest resolution. Runtime depends on both the number of tiles (432 small and 48 large per channel) and the tile dimensions (194 × 459 × 303 and 194 × 1377 × 909 voxels per channel).